JOURNAL OF MATERIALS SCIENCE 22 (1987) 407–414

Microstructure of Y-PSZ after ageing at high temperature

TAKAKI MASAKI
Technical Development Department, Toray Industries Inc., Otsu Shiga 520, Japan
YUKIO MURATA
Toray Research Centre Inc., Otsu Shiga 520, Japan

Partially stabilized zirconia (PSZ) materials containing 2.5 and 5.0 mol% Y_2O_3 were prepared by pressureless sintering and aged at 1200° C for 1000 h, and their microstructures were analysed by transmission electron microscopy and electron diffraction methods. Tetragonal zirconia polycrystal (TZP) containing 2.5 mol% Y_2O_3 before ageing showed nearly 100% tetragonal microstructure and 0.5 μm grain size, but after ageing the microstructure changed greatly, exhibiting no simple grain structure over wide areas. Repeated twin structures within the grains were observed. Y-PSZ material containing 5.0 mol% Y_2O_3 before ageing showed a tetragonal (t) structure within a cubic (c) stabilized ZrO_2 matrix. After ageing, structures of fine strip crystals crossed each other orthogonally within the cubic matrix and typical diffuse scattering in the diffraction pattern was observed. Repeated twins were found on the plane of $(1\,0\,0)_m$, and the orientational relationship between tetragonal (t) and monoclinic (m) crystal was determined to be $(1\,0\,0)_m \parallel (1\,0\,0)_t$, $[0\,1\,0]_m \parallel [0\,0\,1]_t$.

1. Introduction

Among the partially stabilized zirconias of the ZrO_2–Y_2O_3 system, tetragonal zirconia polycrystal (TZP) of nearly 100% tetragonal structure is drawing attention as a material having both high strength and toughness [1, 2]. The high toughness of Y-TZP material is considered to be caused by the martensitic transformation from tetragonal to monoclinic symmetry occurring near the propagating cracks and by the transformation related to the volume expansion [3]. Therefore, to obtain a toughened zirconia depends on the production of a sintered material by stabilizing zirconia of tetragonal structure at room temperature. Manufacturing conditions, such as powder properties or purity, composition of Y_2O_3 or additives, and sintering conditions have a great influence on stability of the tetragonal structure of sintered ZrO_2 material.

A study of the microstructure of the sintered material is indispensable and intensive work is being carried out on not only the matrix structure, intragranular precipitates, and microstructure near the grain boundary, but also into the transformation from t to m symmetry [4–6].

Of the high toughened zirconias, PSZ is divided into two types by the tetragonal formation method: the sintered polycrystalline type of ZrO_2–Y_2O_3 [7] and the precipitate type represented by the ZrO_2–MgO [8] or – CaO [9] system. Their microstructures have been widely studied.

Using powders of high purity, we have prepared sintered Y-PSZ materials containing 2.5 and 5.0 mol% Y_2O_3 by pressureless sintering. Changes in the microstructures were analysed after ageing the sintered materials at 1200° C for 1000 h. In this paper we report the results of the microstructure of sintered materials and precipitates within grains, observed by electron microscopy by the bright-field and dark-field methods, and the crystal lattice structures of t and m analysed by selected-area electron diffraction.

2. Experimental procedure

Zirconias containing 2.5 and 5.0 mol% Y_2O_3 were formulated. Predetermined compositions were prepared using $ZrOCl_2$ from 99.9% ZrO_2 and YCl_3 from 99.5% Y_2O_3 as starting material. The mixing solution was thermally decomposed, calcined at 1000° C for several hours, ground in water using zirconia balls in a mill lined with polyurethane, and dried.

In pressureless sintering, the powder obtained was isostatically pressed into a sample 40 mm wide, 30 mm thick, and 50 mm long at a pressure of 200 MPa. The sample was then heated from room temperature to 900° C at a rate of 50 to 100° C h^{-1} and from 900 to 1500° C or 1550° C at a rate of 30° C h^{-1} and held at this temperature for 2 h, then cooled at a rate of

TABLE I Chemical analysis of 2.5 mol% Y_2O_3 zirconia powder and material sintered at 1500° C

	Powder (wt%)	Sintered material (wt%)
SiO_2	0.016	0.026
Al_2O_3	0.020	0.040
Fe_2O_3	0.005	0.008
Na_2O	0.030	< 0.02
MgO	< 0.001	< 0.001
CaO	0.032	0.025
TiO_2	0.021	0.016
Y_2O_3	4.52	4.41
HfO_2	2.65	2.85

0022–2461/87 $03.00 + .12

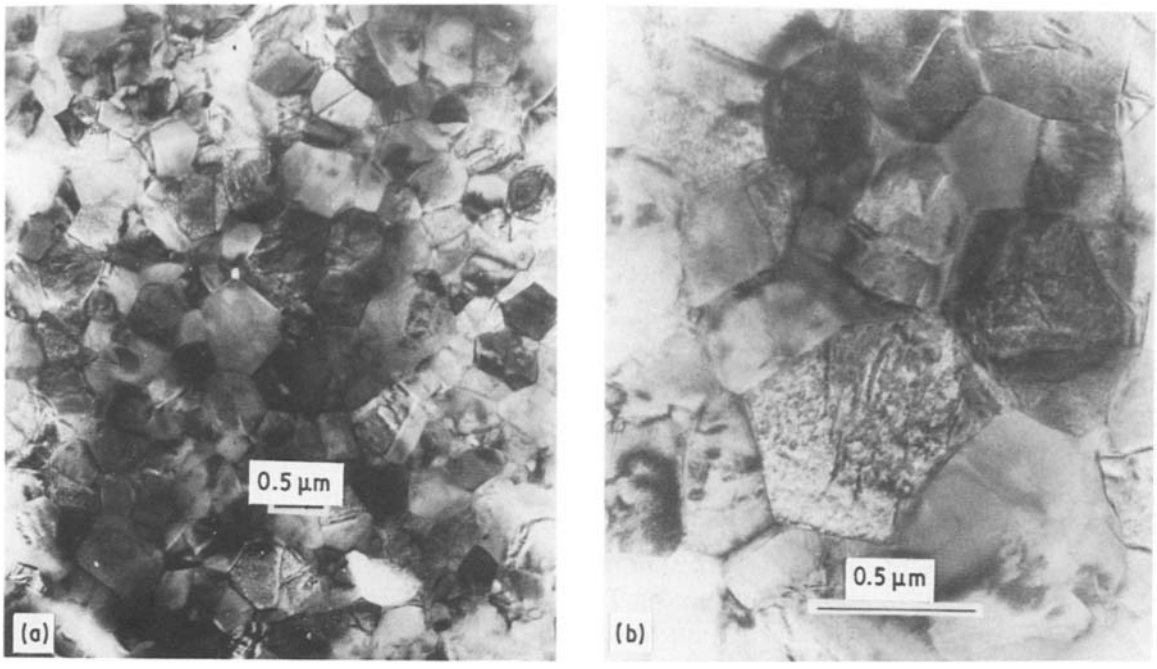

Figure 1 Structure of 2.5 mol % Y-TZP sintered at 1500° C. (a) Electron microscopic structure. (b) Magnified view, showing fine and dense textures.

250° C h^{-1} to 1000° C, 200° C h^{-1} from 1000 to 600° C and subsequently air-cooled; a sintered material was obtained. The densified Y-PSZ samples were aged for 1000 h in air at 1200° C in an electric furnace.

The microstructure of the sample before and after ageing was observed by transmission electron microscopy (Model H-600, Hitachi, 100 kV). A thin film was prepared by means of normal ion-thinning (Gatan 600 C).

To identify the crystal structure of the sintered material and the crystal lattice relationship between t, c and m, a gold standard sample was used and analysed by selected-area electron diffraction.

The twins within the grains and the new crystal phase were analysed by high resolution electon microscopy (Model H-800, Hitachi, 200 kV). The ZrO_2–Y_2O_3 powder and sintered materials were analysed by the inductively coupled plasma (ICP) emission technique.

Table I shows the chemical analysis of the raw powder and material sintered at 1500° C. Although 0.03% Na_2O is present, it decreases to less than 0.01% by evaporation during sintering, although impurities such as Fe_2O_3, SiO_2 and Al_2O_3 are introduced by processing, and hence the purity of the powder is about 99.9%, including ZrO_2 and HfO_2.

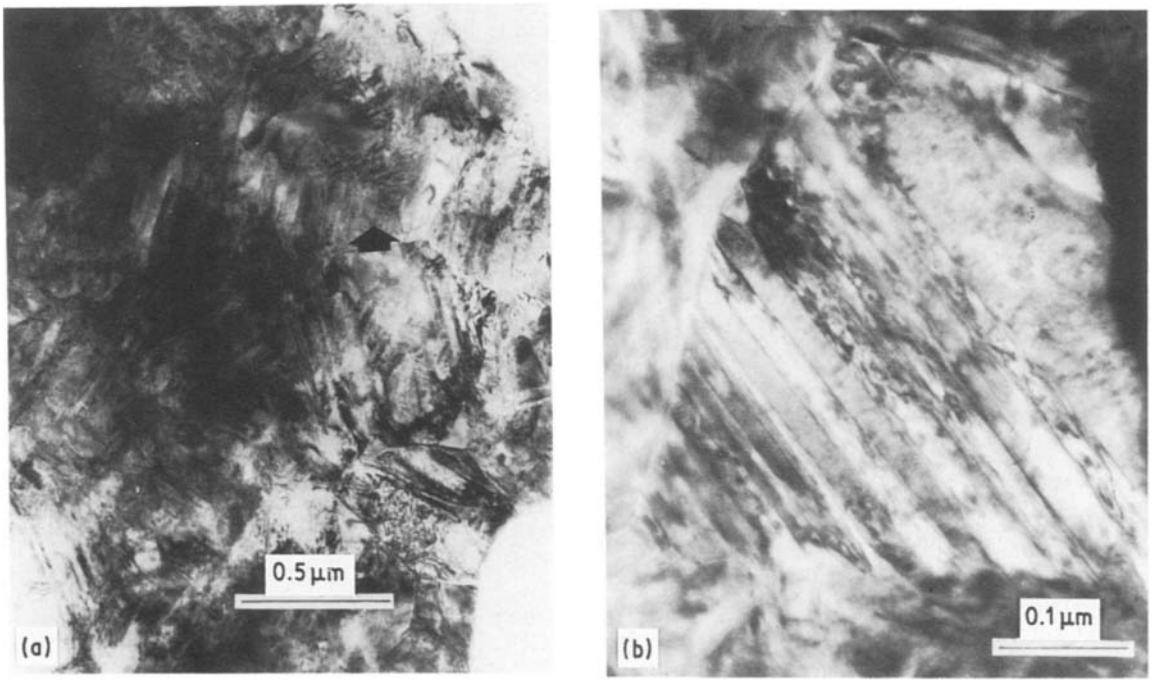

Figure 2 Structure of 2.5 mol % Y-TZP after ageing. (a) Electron microscopic structure; almost no grains are observed, and plate-like crystals and cracks are detected (arrow). (b) Repeated twins within grains.

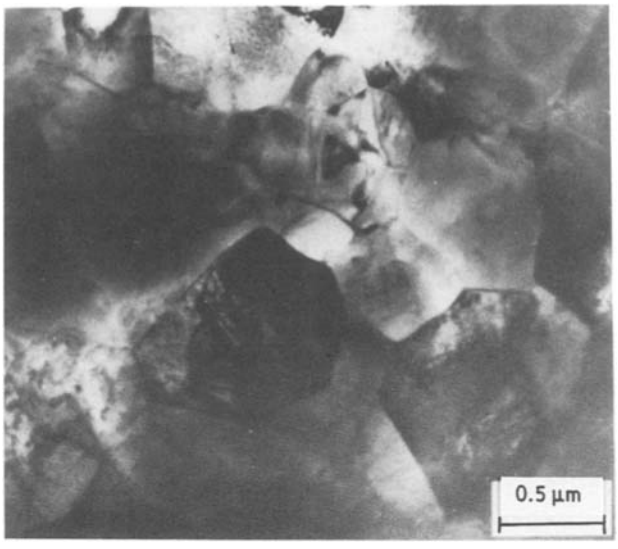

Figure 3 Structure of 5.0 mol % Y-PSZ sintered at 1500° C. Electron microscopic picture; grain sizes are not uniform, and particles of up to 3 μm are present.

3. Results and discussion

3.1. Structure of the sintered material

Figs 1 and 2 show the electron micrographs of 2.5 mol % Y-TZP material sintered at 1500° C before and after ageing at 1200° C for 1000 h, respectively. Fig. 1a shows the general aspect of the grains of about 0.5 μm diameter. Triple point micropores still remain, but the grain size is mostly fine and they are densely sintered as shown in Fig. 1b.

The structure after ageing is shown in Fig. 2, in which almost no simple grain structure exists. The formation of plate-like crystals, a fine structure with a striped pattern in a complicated manner as indicated by the arrow in Fig. 2a, and repeated twins as shown in Fig. 2b, are observed over the whole area. Thus the influence of ageing is quite remarkable.

Figs 3 and 4 show electron micrographs of 5.0 mol % Y-PSZ material sintered at 1500° C before and after ageing at 1200° C for 1000 h. In Fig. 3 grain sizes are not uniform, with a distribution range of 0.4 to 1 μm, and grains of several micrometers are also observed.

Fig. 4 shows the microstructure within the grains of 5.0 mol % Y-PSZ material after ageing at 1200° C for 1000 h. The characteristic feature of mutually crossed fine strip crystals is clearly observed in Fig. 4a; this is called a tweed pattern or modulated structure. A dark-field image of the same view is shown in Fig. 4c. The apparent difference between the bright field and dark field is observed. The dark-field image is similar to the patch structure observed in Fig. 3c, but the patch size grows slightly. From two images, it is realized that the strip-shaped fine structure, as shown in Fig. 4b, and the fine patch structure are superposed within the matrix after ageing.

In PSZ materials, microstructures after ageing have been actively studied [8–10]. Hannink [11] and others observed the morphologies of tetragonal zirconia in PSZ, and found the cause of tweed pattern or

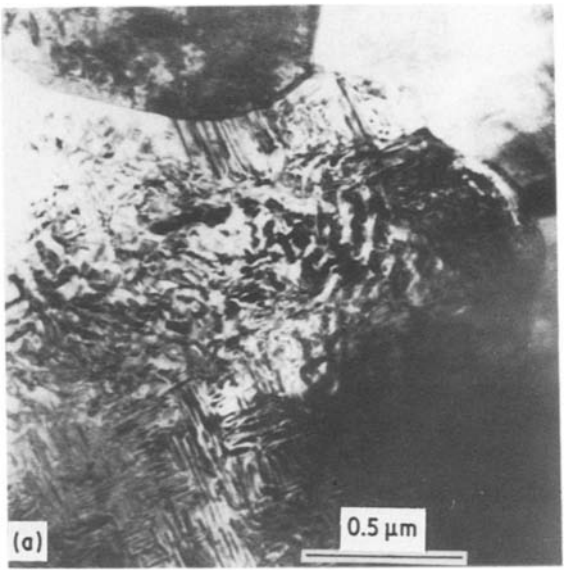

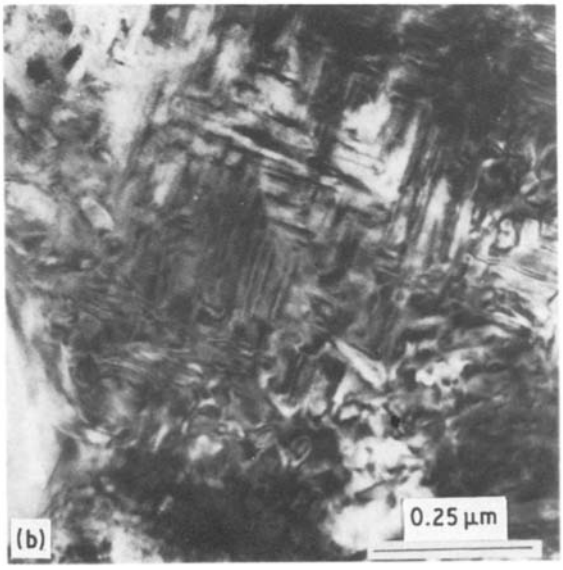

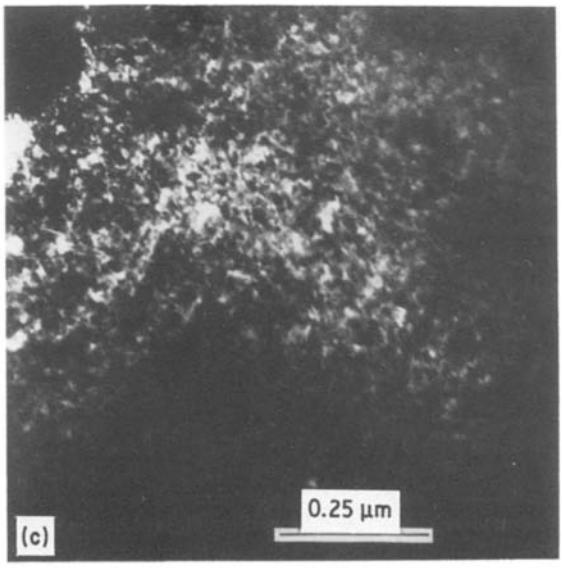

Figure 4 Structure of 5.0 mol % Y-PSZ after ageing. (a) Magnified view within a grain; strip-shaped fine crystals orthogonally cross each other. (b) Magnified view of (a). (c) Dark-field image of (b); a structure similar to Fig. 3c is observed.

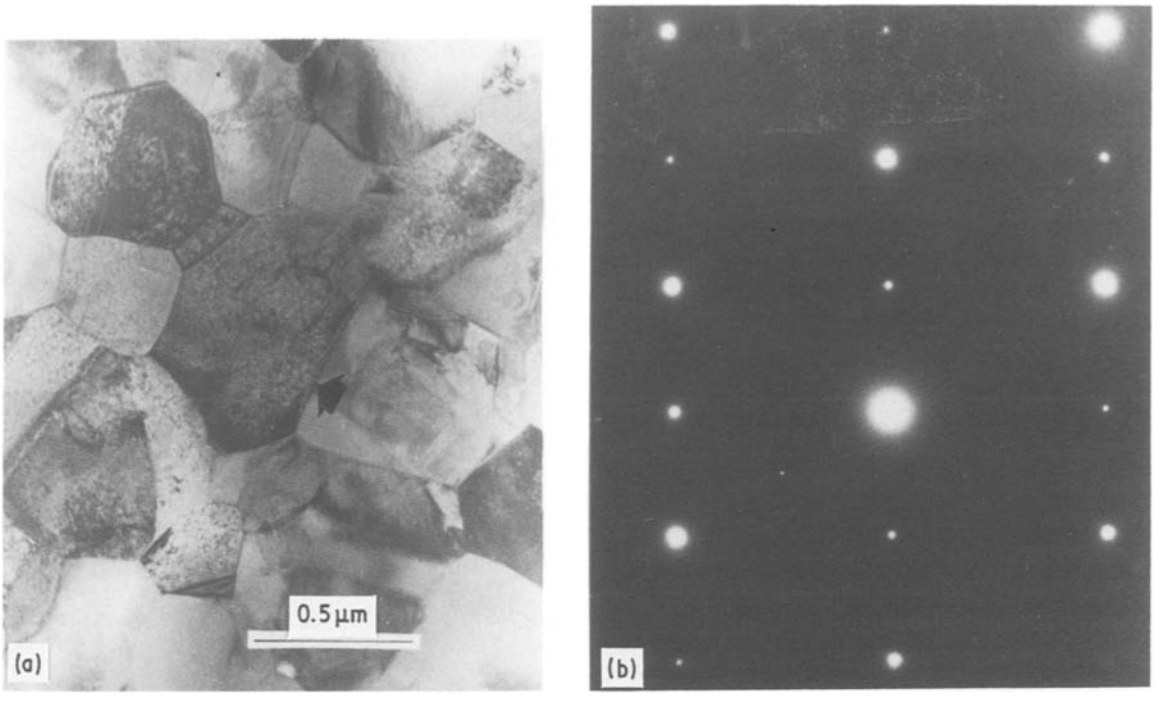

Figure 5 Electron micrograph and electron diffraction pattern of 2.5 mol % Y-TZP sintered at 1500° C. (a) Structure of sintered material. (b) Diffraction pattern from the arrowed area in (a): tetragonal structure is shown.

modulated structure to be the difference in the lattice constant between the cubic and tetragonal structure, and explained that these structures were formed by the growth or gathering of tetragonal domains within the cubic matrix. Later, Valentine *et al.* [12] classified 12 kinds of fine tertagonal precipitates of 4.5 mol % Y-PSZ material after ageing at 1500° C, and discovered that there was a {1 1 0} crystal habit plane. They also reported that the structure was composed of plate-shaped or spherical precipitates, and a fine structure of tweed pattern made of very small tetragonal particles. These microstructures are similar to that observed in Fig. 4a, and the orthogonal crossing between strip-shaped crystals shows particularly characteristic features.

3.2. Identification of crystals

Figs 5 and 6 show the electron micrograph and electron diffraction pattern of 2.5 mol % Y-TZP material sintered at 1500° C before and after ageing, Fig. 5b shows the diffraction pattern from the [1 1 0] orientation obtained from one particle in Fig. 5a, showing the mainly t structure. The diffraction pattern after ageing at 1200° C for 1000 h is shown in Fig. 6 together with the intragranular structure. Fig. 6b shows the high resolution micrograph taken from the middle part of Fig. 6a in which the repeated twins are observed. In Fig. 6c, a selected-area electron diffraction pattern from the middle part of Fig. 6a is shown, and the results of analysis illustrate the coexistence of three phases of t, c and m, although the intensity of diffraction spots from t is very faint. Fig. 6d illustrates schematically one orientational relationship. Superposition of Fig. 6d in a perpendicular manner simulates an actual diffraction pattern as shown in Fig. 6c. The existence of t phase is determined from the diffraction spots of the (2 2 0) and (0 0 2) planes.

Fig. 7 shows the selected-area electron diffraction image of 5.0 mol % Y-PSZ material sintered at 1500° C before and after ageing. Both Figs 7a and b show the results of Y-PSZ before ageing, and Fig. 7a shows the diffraction image from [1 1 1] orientation, in which the t-phase within the c-ZrO_2 matrix is recognized from the split of the diffraction spot. Fig. 7b shows the diffraction pattern from a particle in Fig. 3, giving fine spot patterns. In addition to the diffraction spots, a broad and band-shaped diffuse scattering is clearly observed.

Rossell [13] reported that the above diffuse scattering appeared due to the formation of a superlattice of $Zr_3Y_4O_{12}$ composition, and that it was caused by heat treatment such as ageing. Thus, its appearance will be due to the disturbance of atomic array within the c-matrix after ageing. Fig. 7c shows the diffraction pattern after ageing, in which a diffraction spot in a regular manner is noted, although the strength is weak. It is presumed that the mutual crossing of strip domains is related, and also complicated diffraction patterns are observed, different from Fig. 7c, and further analyses will be required.

3.3. Orientational relationship between t and m symmetry

Twins of plate-shaped crystals are shown in Fig. 2b, while Fig. 8 shows an example of characteristic twins of 2.5 mol % Y-TZP material sintered at 1500° C, in which coexistence of m- and t-phases was observed. As shown in Fig. 8a, the pattern of each fine crystal is close to the similar parallelogram, and its quadilateral orientation is inverted from the twinning plane and is continuously developed. The regular contrasts of the quadrilateral pattern show dense and pale parts; the dark portion satisfies the Bragg condition. The formation of cracks near the apex of the quadrilateral shape

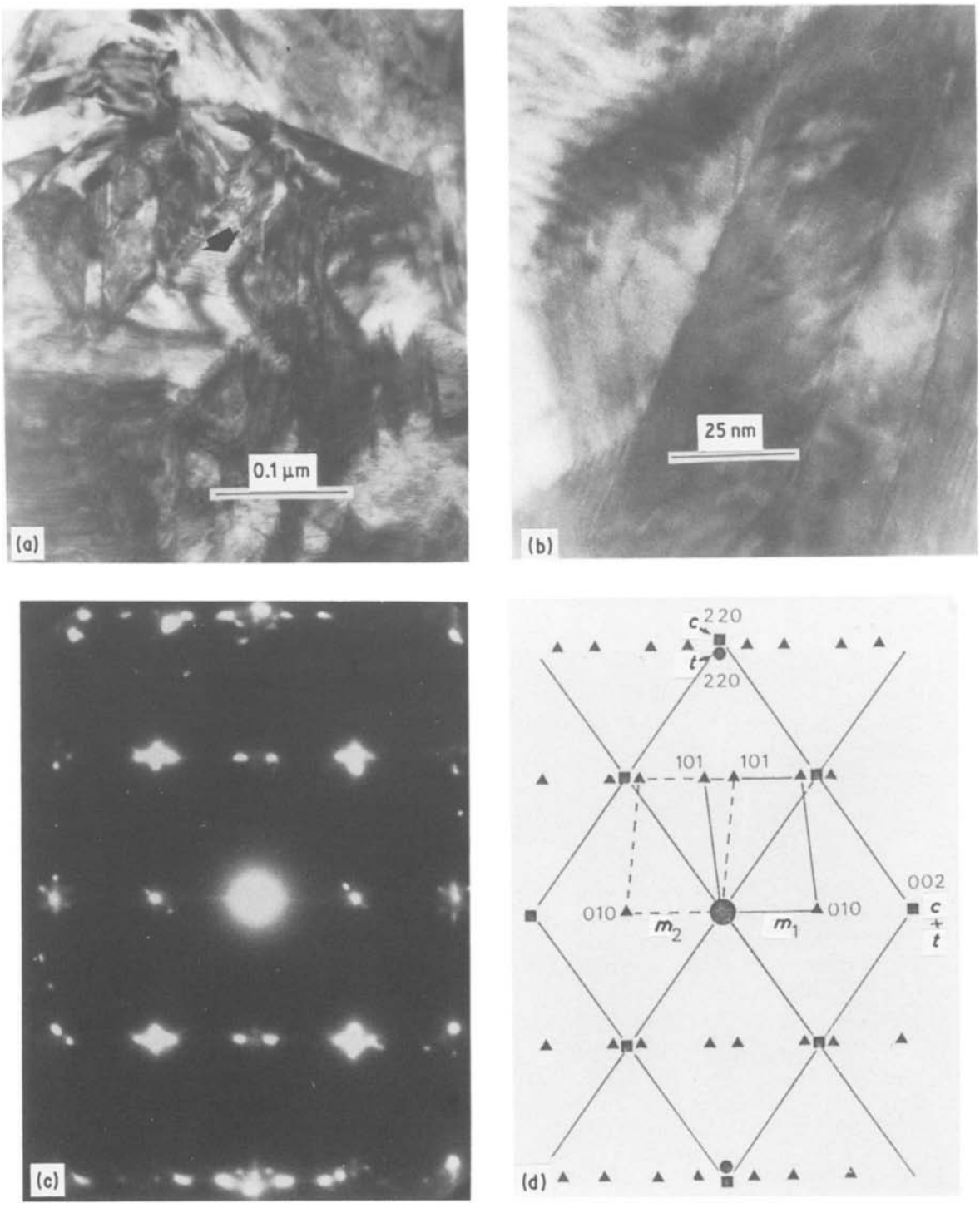

Figure 6 Electron micrograph and electron diffraction pattern of 2.5 mol % Y-TZP sintered at 1500° C after ageing. (a) Structure within grains; repeated plate-shaped crystals are noted. (b) High resolution micrograph of middle part (arrow) in (a). (c) Selected-area electron diffraction image in (a); many faint traces of diffraction lines are observed. (d) A model diagram of the above analysis showing the coexistence three phases of c, m and t. The reciprocal lattice points are shown by ■ = c, ● = t and ▲ = m.

is caused by the volume expansion due to the transformation from t to m symmetry. A diffraction pattern from this repeated twinning part and a model diagram are shown in Figs 8b and c. In Fig. 8c, the coexistence of t- and m-phases is recognized, and two diffraction spots of m-phase differring in its orientation are superposed, which correspond to two types possessing density contrast. One of the diffraction spots of m-phase is indicated by ▲, the other by ●, and the diffraction point of t-phase is represented by ■. In both diffraction spots of the m-phase, the a^*c^* plane (a^*, c^* are reciprocal lattices) is parallel to the paper surface, and the *b*-axes of the twin are parallel to each other. As a result the twin relationship of $(1\,0\,0)_{m1} \parallel (1\,0\,0)_{m2}$ and $[0\,1\,0]_{m1} \parallel [0\,1\,0]_{m2}$ is obtained, and the angle formed by c^*_{m1} and c^*_{m2} is 140 degrees. Since $(1\,0\,0)_m$ or $(2\,0\,0)_m$ and $(1\,0\,0)_t$ or $(2\,0\,0)_t$ appears on the same axis, the plane relationship becomes $(1\,0\,0)_m \parallel (1\,0\,0)_t$. Since $(0\,1\,0)_t$ of the t-phase is analysed, it is the projection of $[0\,0\,1]_t$ of the t-phase. a^* c^* of the m-phase is parallel to the paper surface and it is the $[0\,1\,0]_m$ projection of the m-phase. As a result, the orientational relationship

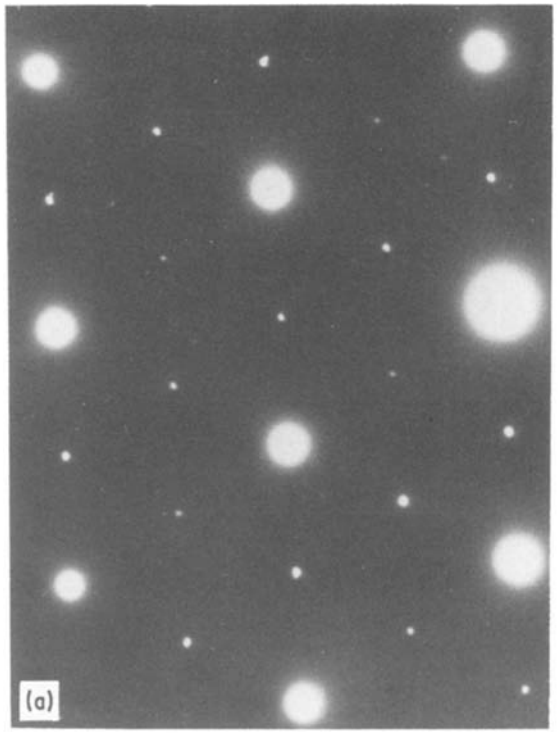

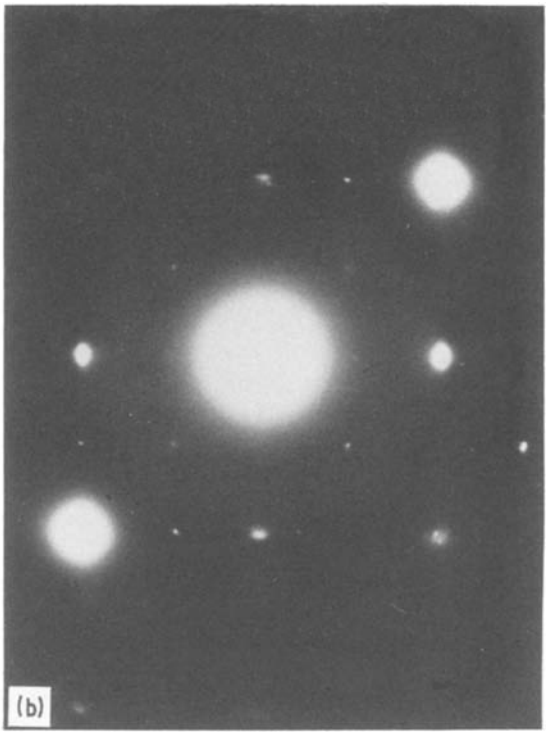

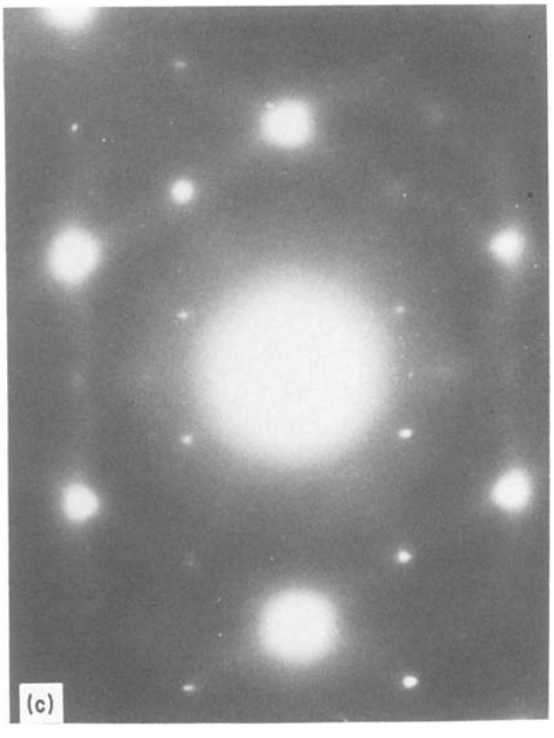

Figure 7 Electron diffraction patterns of 5.0 mol % Y-PSZ before and after ageing. (a) Diffraction pattern before ageing; t-phase coexists within the c-matrix. (b) Diffraction pattern before ageing; band-like diffuse scattering is noted. (c) Diffraction pattern after ageing; regular scattering, estimated to correspond to the strip crystals in Fig. 4a is recognized.

between the t- and m-phases is

$$(1\,0\,0)_m \parallel (1\,0\,0)_t,\ [0\,1\,0]_m \parallel [0\,0\,1]_t.$$

This agrees with the relation discovered by Bansal and Heuer [14, 15] at temperatures above 1000° C.

In the actual diffraction pattern as shown in Fig. 8b, many total reflection patterns are observed apart from the model diffraction image as shown in Fig. 8d. For example, as shown in Fig. 8d, there appear four satellite spots in the periphery of the principal diffraction point. Their appearance will be due to the double diffraction caused by the overlapping of m and t crystals.

3.4. Formation of a new crystal phase

Apart from the diffuse scattering in 5.0 mol % Y-PSZ as mentioned before, an example of the formation of a new crystal phase in 2.5 mol % Y-TZP sintered at 1550° C is shown in Fig. 9. When the electron irradiation in weak, the long streak extended toward the [1 0 0] direction is clearly observed, as shown in Fig. 9b. After intense irradiation, however, the long streak becomes strong in diffraction intensity and short, elongated spots develop, as shown in Fig. 9c. The diffraction spots indicated by an arrow in Fig. 9c correspond to a planar distance of 1 nm in real space. However, such a lattice plane corresponding to 1 nm cannot be assigned to any crystals of the c, t and m phases. There is a possibility of a double diffraction effect for the appearance of extra spots in a thick specimen and for such a case, the extra spot is not formed in the manner of the characteristic streak as seen in Fig. 9. Therefore, the appearance of the extra spot is not due to a dynamical effect, but to the formation of a new crystal phase induced by intense electron irradiation for the metastable region. From the above, it is considered the new crystal phase has a two-fold t lattice in the [1 0 0] direction.

Fig. 9d shows a high resolution electron micrograph of Fig. 9a. As apparent, a fringe with a 1 nm interval which corresponds to the extra elongated spots (Fig. 9c), is observed in nearly regular manner. The 1 nm fringe does not appear in the entire view, and it is not clear. The portion in which the lattice irregularly

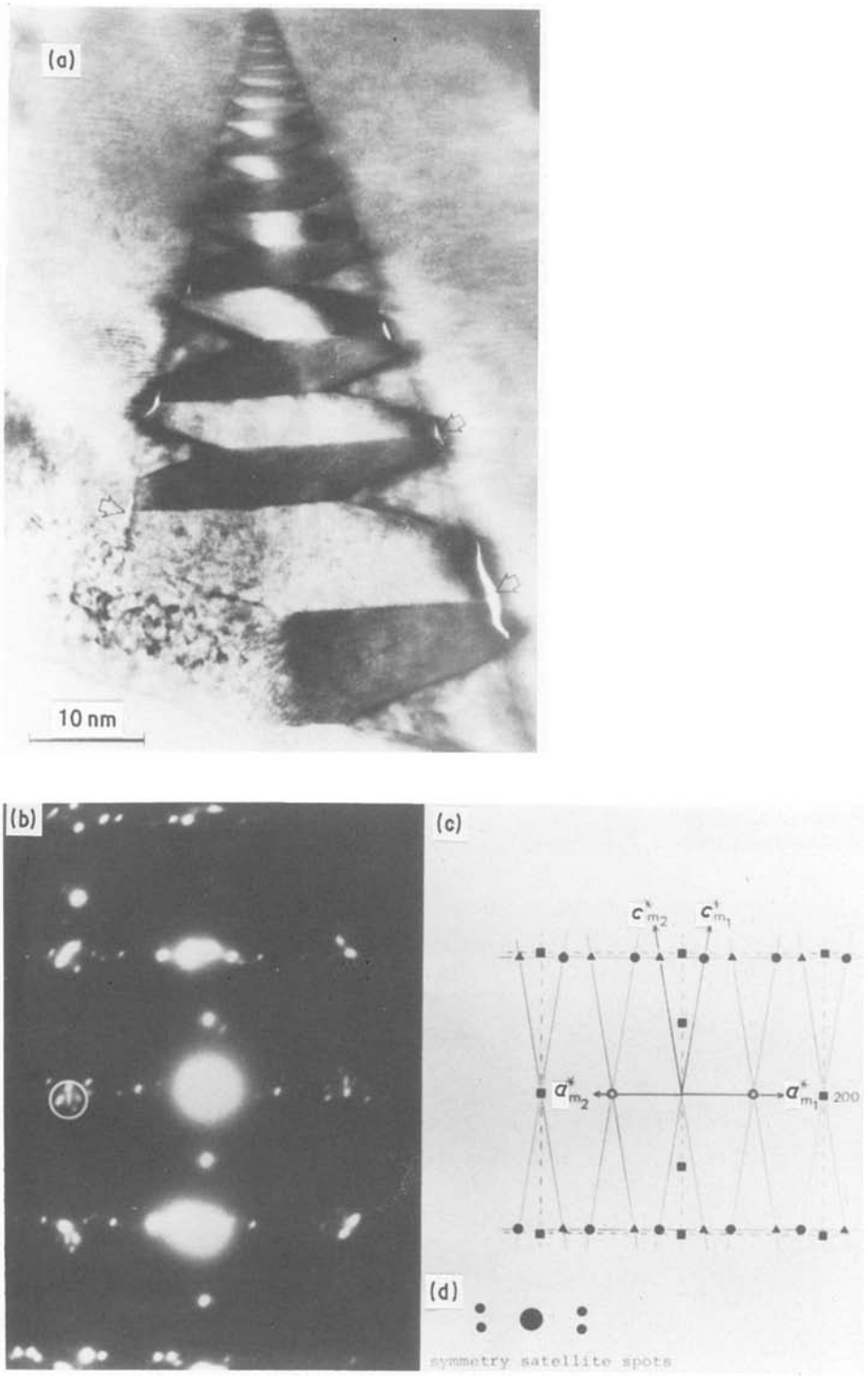

Figure 8 Electron micrograph and electron diffraction pattern of parts within a grain of 2.5 mol % Y-TZP sintered at 1500° C. (a) Electron micrograph: repeated twins and growth of cracks (arrows) are noted. (b) Selected-area electron diffraction pattern obtained from (a). (c) Analytical results of (b). (d) Model diagram of symmetry satellite.

disappears may be due to the original t phase. In this micrograph, the 0.25 or 0.5 nm lattice fringe of t is not resolved. Even after intense irradiation the extra spot is still seen in the streak, therefore it is assumed that the new phase is not perfect in the sense of a single crystal.

Acknowledgement

The authors thank Mr T. Nagato and Mr Y. Ueda at the Technical Development Department of Toray Industries, Inc and Mr S. Horii of Toray Research Centre for their contribution to the preparation of sintered materials and the observation of microstructure in this experiment.

References

1. K. KOBAYASHI and T. MASAKI, *Bull. Jpn Ceram. Soc.* **17** (1982) 427.
2. K. TSUKUMA, Y. KUBOTA and T. TSUKIDATE, in "Advances in Ceramics", Vol. 12, edited by N. Claussen, M. Rühle, A. H. Heuer (The American Ceramic Society, Columbus, Ohio, 1984) pp. 382–90.
3. R. McMEEKING and A. G. EVANS, *J. Amer. Ceram. Soc.* **65** (1982) 242.
4. R. H. J. HANNINK and M. V. SWAIN, *J. Aust. Ceram. Soc.* **18** (1982) 53.
5. A. H. HEUER, in "Advances in Ceramics", Vol. 3, edited by A. H. Heuer and L. W. Hobbs (The American Ceramics Society, Columbus, Ohio, 1981) pp. 98–115.
6. N. CLAUSSEN, in "Advances in Ceramics", Vol. 12, edited by N. Claussen, M. Rühle, A. H. Heuer (The

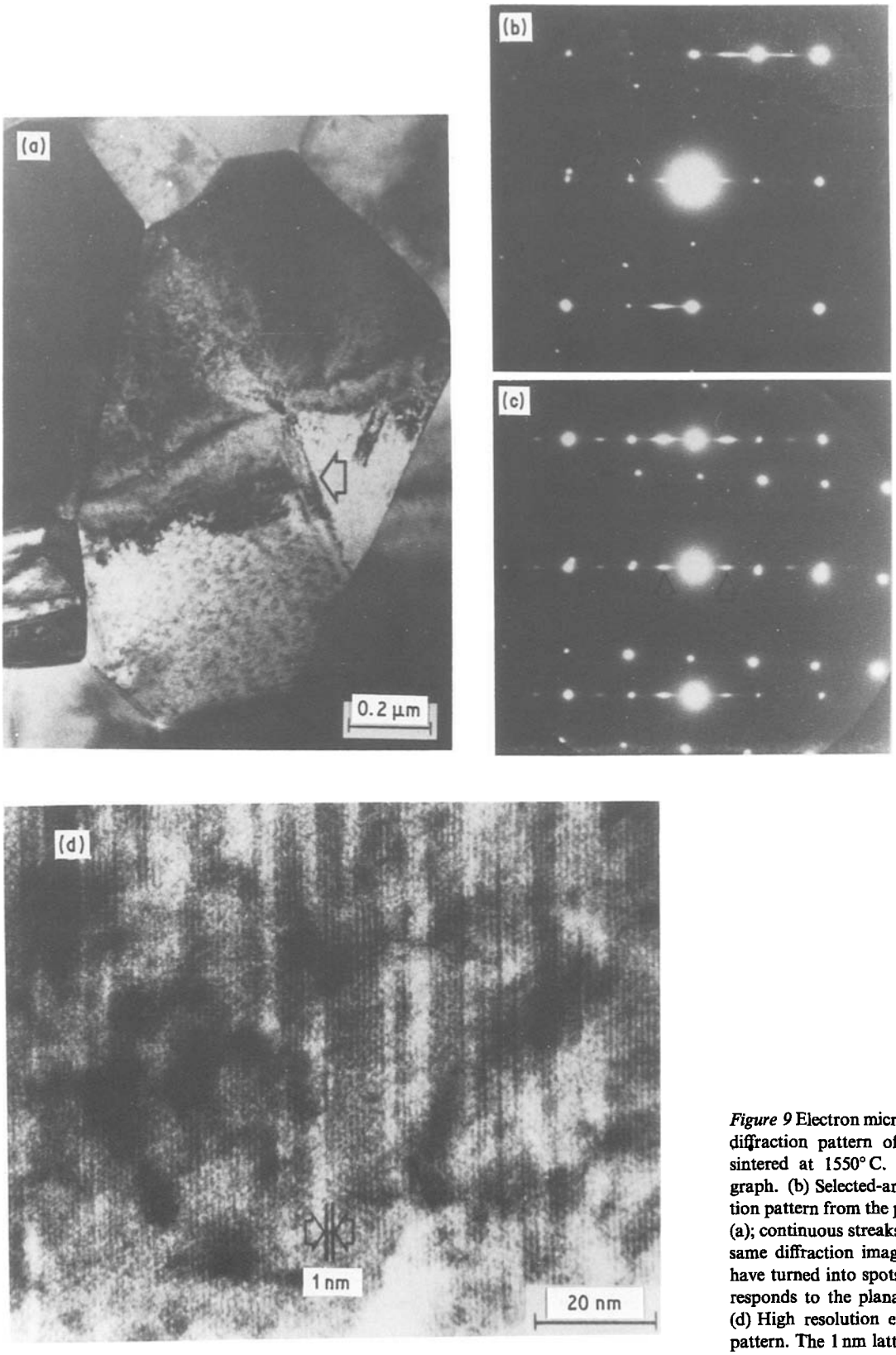

Figure 9 Electron micrograph and electron diffraction pattern of 2.5 mol % Y-TZP sintered at 1550° C. (a) Electron micrograph. (b) Selected-area electron diffraction pattern from the particle (arrowed) in (a); continuous streaks are shown. (c) The same diffraction image as in (b); streaks have turned into spots, and one spot corresponds to the planar distance of 1 nm. (d) High resolution electron microscopic pattern. The 1 nm lattice is observed.

American Ceramics Society, Columbus, Ohio, 1984) pp. 325–51.
7. C. A. ANDERSSON, J. GREGGI Jr and T. K. GUPTA, in "Advances in Ceramics", Vol. 12, edited by N. Claussen, M. Rühle A. H. Heuer (The American Ceramics Society, Columbus, Ohio, 1984) pp. 78–95.
8. D. L. PORTER and A. H. HEUER, *J. Amer. Ceram. Soc.* **62** (1979) 298.
9. R. C. GARVIE, R. H. J. HANNINK, R. R. HUGHAN, N. A. McKINNON, R. T. PASCOE and R. K. STRINGER, *J. Aust. Ceram. Soc.* **13** (1977) 8.
10. T. SAKUMA, Y. YOSHIZAWA, H. SUTO, *J. Mater. Sci. Lett.* **4** (1985) 29.
11. R. H. HANNINK, *J. Mater. Sci.* **13** (1978) 2487.
12. P. G. VALENTINE, R. D. MAIER and T. E. MITCHELL, National Aeronautics and Space Administration Grant No. NSG-3252 (1981).
13. H. J. ROSSELL, in "Advances in Ceramics", Vol. 3, edited by A. H. Heuer and L. W. Hobbs (The American Ceramics Society, Columbus, Ohio, 1981) pp. 47–63.
14. G. K. BANSAL and A. H. HEUER, *Acta Metall.* **20** (1972) 1281.
15. *Idem, ibid.* **22** (1974) 409.

Received 3 February
and accepted 22 May 1986